Chapter 6

Utilization of E-waste by single-step reactive extrusion

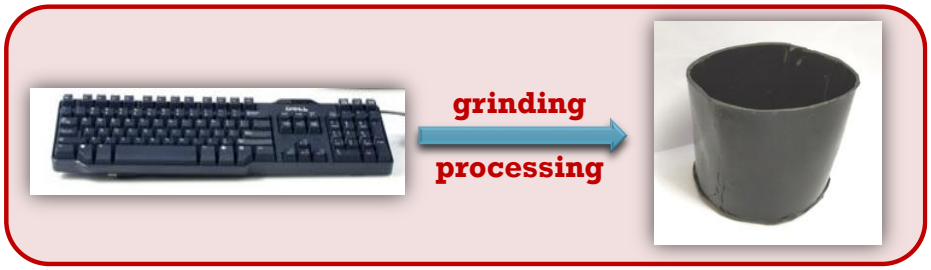

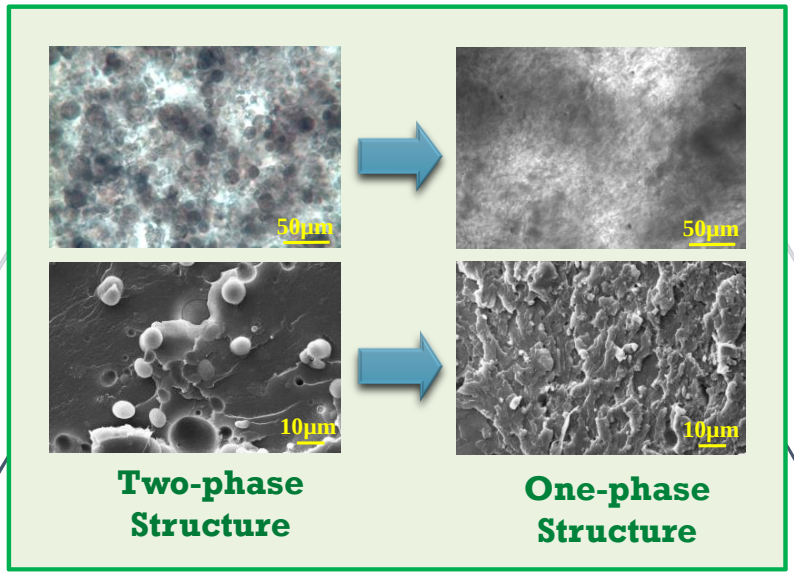

Chapter 6

6.1 Introduction

The plastic-waste is prevailing and piling up since there is too much plastic that is discarded everyday in different fields. One of the segment which generate large amount of plastic waste is electronic waste or E-waste. The solution to this problem is to utilize this waste into producing useful material for practical purposes as polymers present in E-waste have great potential to be modified and re-used.

To incorporate the desirable properties, there arises a need to improve the belongings for different specific applications. Making polymer composites by using different kinds of filler is a well-known method to improve various properties such as structural, thermal, mechanical, gas barrier as well as in the field of biomedical, fuel cell applications etc. [20, 170, 238]. Other popular technique is to combine different polymers for the required purpose and making polymer blends. The polymer blends have been a widely studied research area. Two or more polymers are combined to modulate and enhance different properties [143, 151, 152, 154, 160, 161, 239, 240]. Polymers having different polarity, which are immiscible as well, needs an additional agent to improve their interfacial interactions [152, 160]. Various kinds of compatibilizers such as LDPE-g-MAH [11], SEBS-g-MAH (styrene-ethylene-styrene copolymer-grafted-maleic anhydride) [160], PP-g-MAH (polypropylene-grafted-maleic anhydride) [151], SEBS [161], PP-g-styrene-*co*-acrylonitrile [154] have been used in the past to improve the morphological, mechanical and other properties of the blends. Use of compatibilizers improve the mechanical properties, reduce the dispersed phase size, improve the interfacial adhesion up to a considerable extent. But the compatibilizers are synthesized

separately which makes the overall process more energy consuming which is commercially undesirable.

Reactive extrusion has been the other technique to prepare polymer blends. In this approach, two polymers and copolymers or functionalized polymers are fed into the extruder and the reaction takes place within the extruder itself [8, 124, 125, 143]. There are two types of reactive extrusions reported; one where the size of dispersed phase is reduced and the reactive agent provides compatibilization and in some reports the reactive extrusion causes crosslinking reactions in the polymer blends which is confirmed by gel content or gel fraction. Vadori *et al.* studied the reactive extrusion of poly(lactic acid) and ABS blends by using two additives (acrylic copolymer and Joncryl) [143]. The morphology of the polymer blend was not changed drastically but the size of the dispersed ABS was reduced and the two-phase morphology persisted. There was improvement in toughness but tensile properties were not improved. Wang *et al.* introduced a two-step crosslinking process for the blends of polystyrene and LDPE [8]. LDPE was partially crosslinked first by using dicumyl peroxide. Then the crosslinked LDPE was melt blended with polystyrene in second step. Styrene-butadiene-styrene was added later in the second step. Mechanical properties were improved due to crosslinking between the two phases. ABS has been used in many studies for making polymer blends for various purposes [5, 124, 125, 143, 152, 160, 163]. There have not been enough research articles on LDPE/ABS system except few [5, 161, 163] due to the fact that the two polymers are highly immiscible and there is a need to modify the blend system. In this study, a one-step reactive extrusion process has been explored to produce a single-phase crosslinked chemical mixture (C-M) of LDPE and ABS in the form of electronic waste. The

C-M has been tested for morphological, mechanical, thermal and heat distortion properties for its applications of reusing plastic E-waste.

6.2 Experimental

6.2.1 Materials: ABS, LDPE, MA.

6.2.2 Preparation of materials

For obtaining the ABS, parts of e-waste (such as computer keyboards, mouse etc) were collected from different sources. These parts were then washed thoroughly to get rid of any dust particles. After drying them, they were dried in air for 24 h and then vacuum dried for another 24 h. The parts were then cut into small pieces and grinded in mechanical grinder for turning them into fine powder. This ABS powder was used for further processing. LDPE granules were also grinded in mechanical grinder for making its fine powder.

6.2.3 Sample preparation

The polymer blends were prepared by melt extrusion technique in twin-screw extruder (Hakke Mini Lab). Fine powder of LDPE and ABS were mixed with MA in different proportions. The optimum ratio of polymers and MA with most favorable temperature conditions were optimized as defined below.

6.2.4 Optimization of blends

6.2.4.1 MA concentration dependence

The blends were prepared for different MA concentration to achieve the optimum MA weight percentage as shown in ***Figure 6.1***. Without MA addition, the physical mixture (P-M) showed a distinct two phase structure as shown in ***Fig. 6.1a***. As 0.75% of MA was added in it, the immiscible structure pertained but there was slight reduction in ABS particle size. As

the blend was continued to test with other MA%, it was found that the 5% of MA showed the best miscible structure.

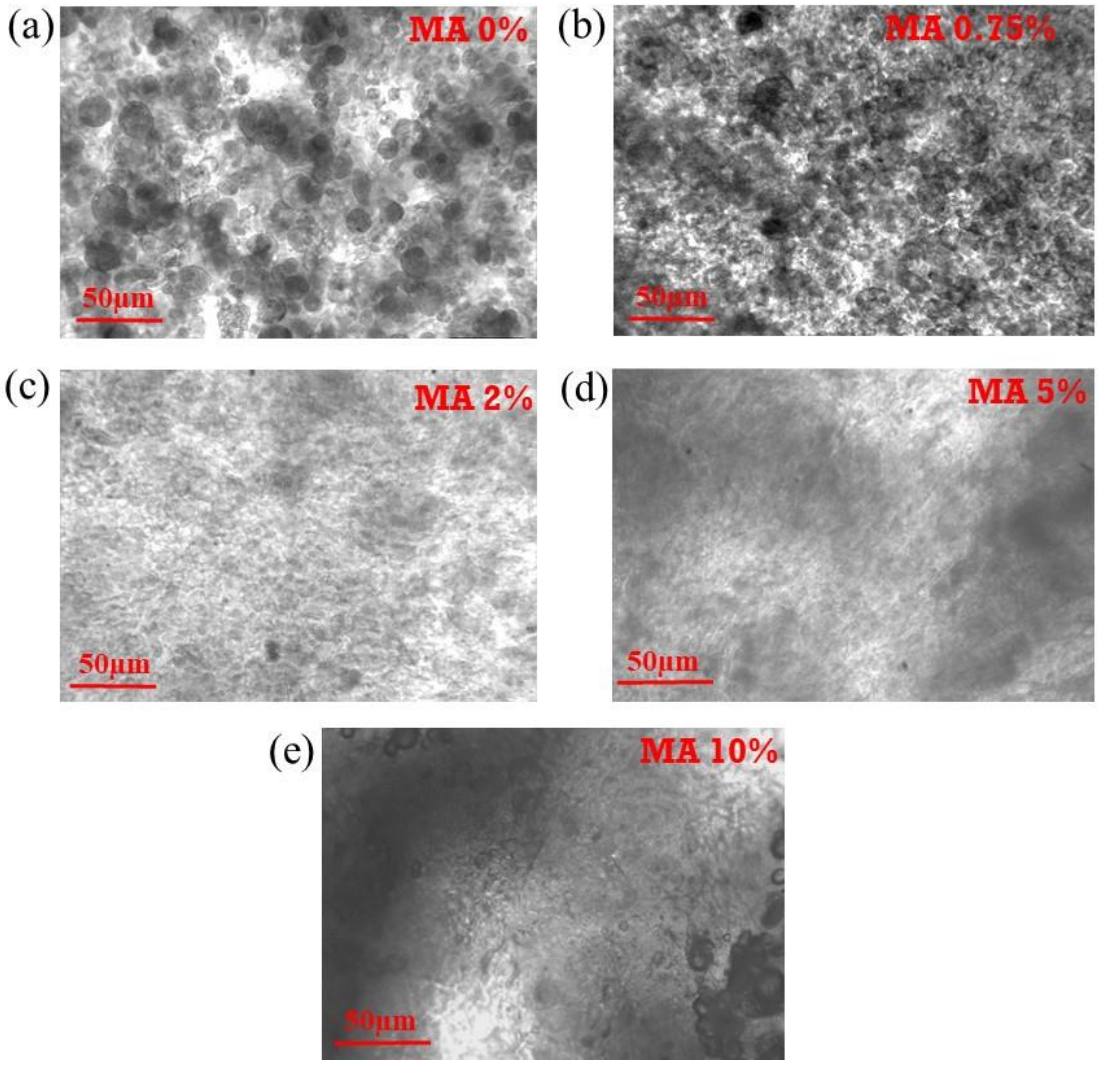

Figure 6.1: *POM images show effect of different MA concentrations of* ***(a)*** *0%;* ***(b)*** *0.75%;* ***(c)*** *2%;* ***(d)*** *5%; and* ***(e)*** *10% on structures of blends containing 75% PE and 25% ABS*

6.2.4.2 Composition dependence

The blends were tested for higher ABS concentration that is 50% and the structures of blends were investigated with and without MA as shown in ***Figure 6.2***. Because of the presence of high amount of ABS (PE:ABS = 50:50), the blend without MA (***Fig. 6.2c***) had large accumulated and highly immiscible portion of ABS. After adding 5% of MA in it, the blend

the blend became miscible to an extent but showed 2-phase structure (***Fig. 6.2d***). Hence, the blend with PE:ABS ratio of 75:25 was selected for further characterizations.

6.2.4.3 Temperature dependence

The effect of temperature variations were also investigated and optimized for PE:ABS= 75:25. Different temperatures taken were 160^{o}C, 190^{o}C and 220^{o}C (***Figure 6.3***). At 160^{o}C, the structure remained same even after adding 5% of MA. At 190^{o}C, the blend containing 5% of MA showed a little miscibility but had large portions of ABS remaining. At 220^{o}C, the blend with 5% MA gave a one phase structure, hence 220^{o}C was taken as the optimum temperature for the processing.

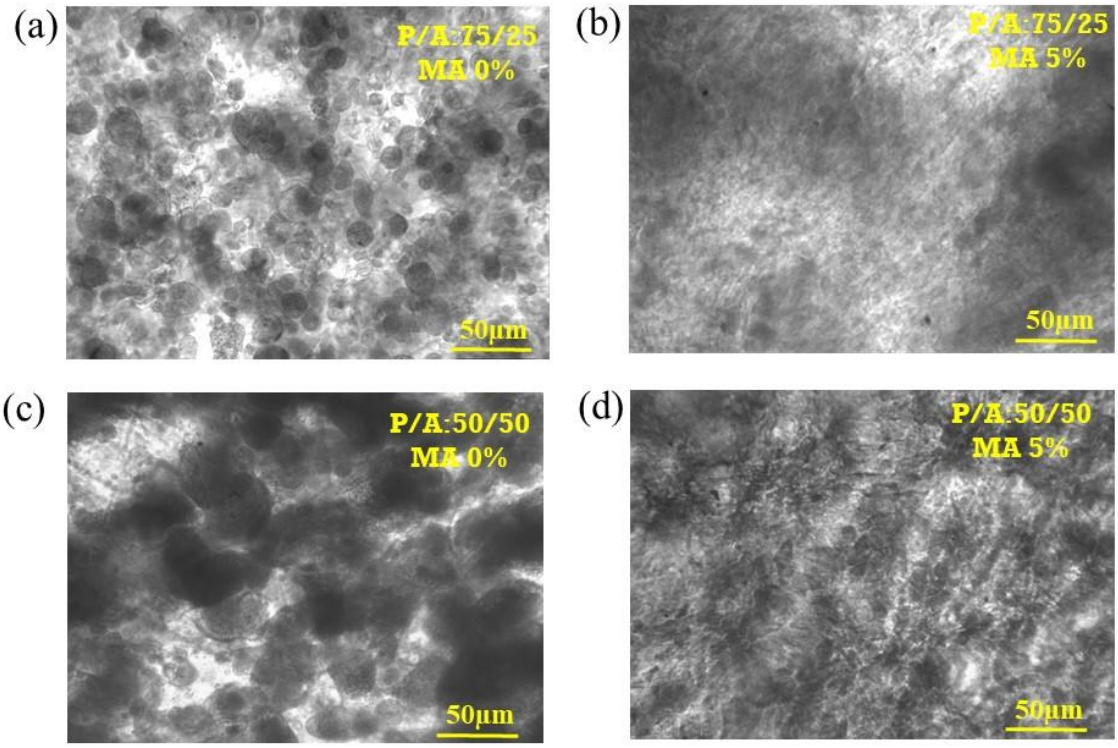

Figure 6.2: *POM images show the effect of varied concentration ratio of PE and ABS (shown as P/A),* ***(a)*** *and* ***(b)*** *has P/A as 75/25 without MA and with 5% MA respectively;* ***(c)*** *and* ***(d)*** *has P/A as 50/50 without MA and with 5% MA concentration respectively.*

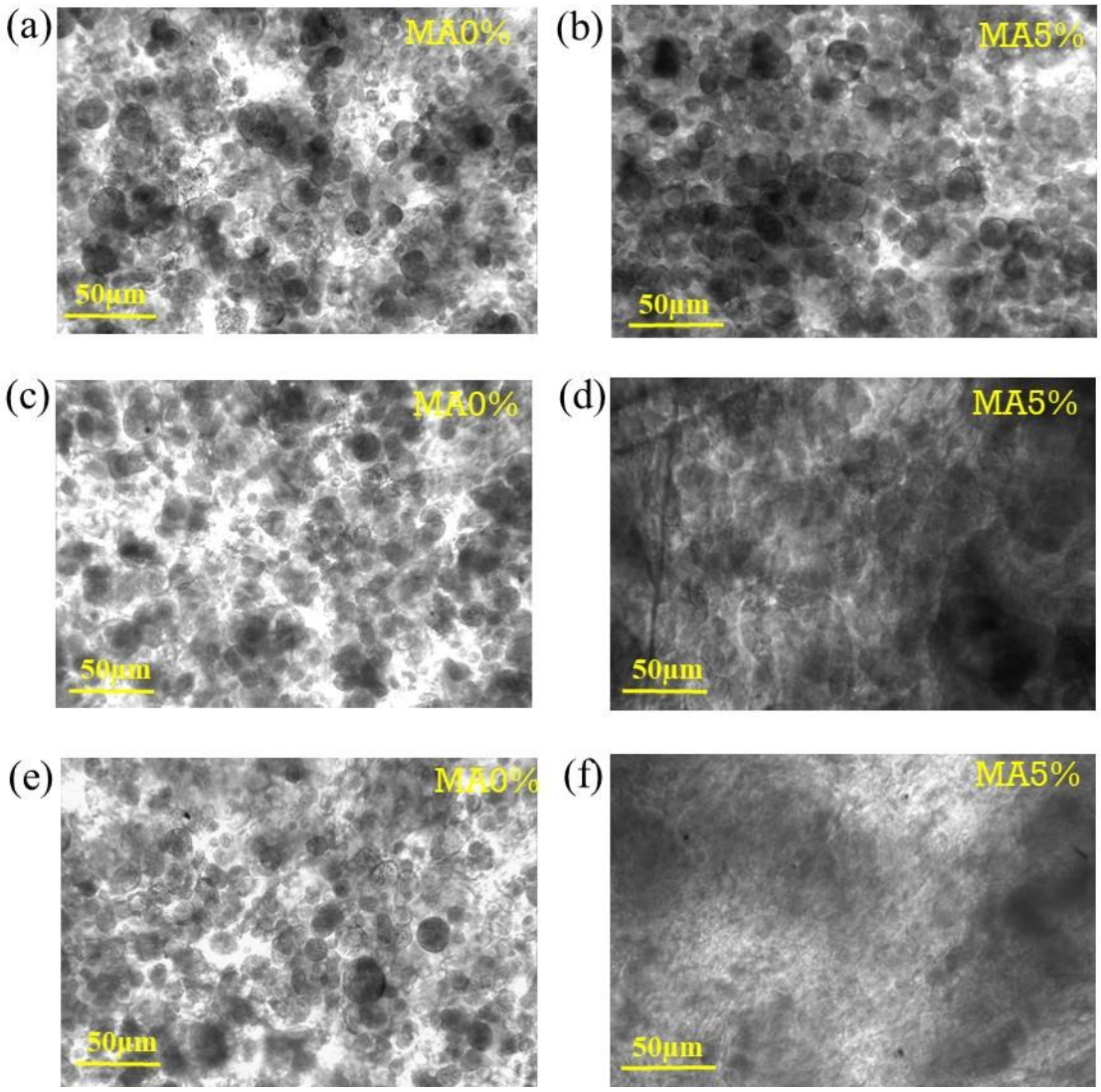

Figure 6.3: *POM images show effect of different temperatures of processing on structure of blends containing 75% PE and 25% ABS; without and with 5% MA.* ***(a)*** *and* ***(b)*** *at 160 °C;* ***(c)*** *and* ***(d)*** *at 190 °C;* ***(e)*** *and* ***(f)*** *at 220 °C.*

Hence, the optimum ratio taken here is PE:ABS as 75:25, MA concentration as 5 wt% and operating temperature as 220 °C. All powders were vacuum dried for 24 h prior to mixing. The blends were processed at a temperature of 220 °C, 100 rpm and a duration of 10 min. Simple mixing of two polymers will be termed as physical mixture (P-M) and the blends

containing 5% of MA will be termed as chemical mixture (C-M) where both blends have 75:25 ratio of PE and ABS. The extruded blends were then made into thin sheets (~20 μm) using compression molding machine (S. D. Scientific Ltd.). These sheets were used for solvent extraction and polarized optical microscopy experiments. The dog bone specimens were also prepared for the mechanical testing using injection molding machine (Haake micro-injector). The polymer blends were heated at 230 °C in the heating barrel. The mold temperature was kept at 40 °C. The material was injected at a pressure of 110 bar. The dimension of hence prepared dog bone samples was: thickness 2.12 mm, gauge length 20 mm and width of 4 mm.

6.2.5 Gel content by solvent extraction

To determine the gel content which is indicative of crosslink density of the polymer blends, solvent extraction experiments were performed. The samples were dipped in solvents of PE and ABS to determine the dissolved percentage of the polymer blends. The samples were cut in a dimension of 1.5 × 1.5 cm^2 having thickness of 20 μm. The samples were weighed before dipping into any solvent. The samples then dipped and stirred in chloroform (solvent of ABS) for 24 h. After 24 h, samples were removed from the solvent and dried in air for 12 h and in vacuum for another 12 h. After that the weight difference was measured. Again the sample was dipped and stirred in xylene (solvent of PE) and the same procedure was repeated. The weight difference was used to determine the crosslinking percentage of the polymer blend.

Gel content (%) = $\frac{W_f}{W_i} \times 100$ = indicative crosslink density (CD_i)

Where, W_f is the weight after solvent extraction and W_i is the initial weight.

The DSC experiments were performed at a temperature range of 25–200 °C after quenching the samples (instrument details mentioned in ***Chapter 2***). The heating rate was kept at 10°/min. Dynamic mechanical properties of the samples were performed on a dynamic mechanical analyzer MCR 702 Multi Drive Anton Paar. The samples' dimensions were taken as 20 × 5 mm^2 having a gauge length of 20 mm and thickness of 1 mm. The samples were tested in torsion mode at a frequency of 1 Hz, temperature range of −50° to 100 °C at a heating rate of 5°/min and strain of 0.05%. SEM, AFM, POM, FTIR, NMR, TGA, tensile test, 3-point bending test and HDT test were performed for the characterizations details of which are mentioned in ***Chapter 2***.

6.3 Results and discussion

6.3.1 Phase morphology

Two immiscible polymers are phase segregated leading to two separate phases. As a result, there is insignificant property development out of mixing the two immiscible polymers. ***Figure 6.4a*** shows the polarized optical micrographs of physical mixture (P-M) and chemical mixture (C-M). The POM images were taken in transmittance mode. The micrograph of P-M shows the two phase system where one phase of ABS is dispersed in the PE matrix. ABS polymer has somewhat spherical morphology which is heterogeneously distributed throughout the polymer blend. On the other hand, the micrograph of C-M exhibits a single-phase morphology which indicates better miscibility of the two polymers. The maleic anhydride (MA) acts as the bonding agent which chemically crosslink the polyethylene (PE) and ABS molecules which eventually convert it into single phase system. Further, the polar interactions between the two polymers enhance in presence of MA. ***Figure***

6.4b shows the SEM images of the fracture surfaces of physical (P-M) and chemical mixture (C-M).

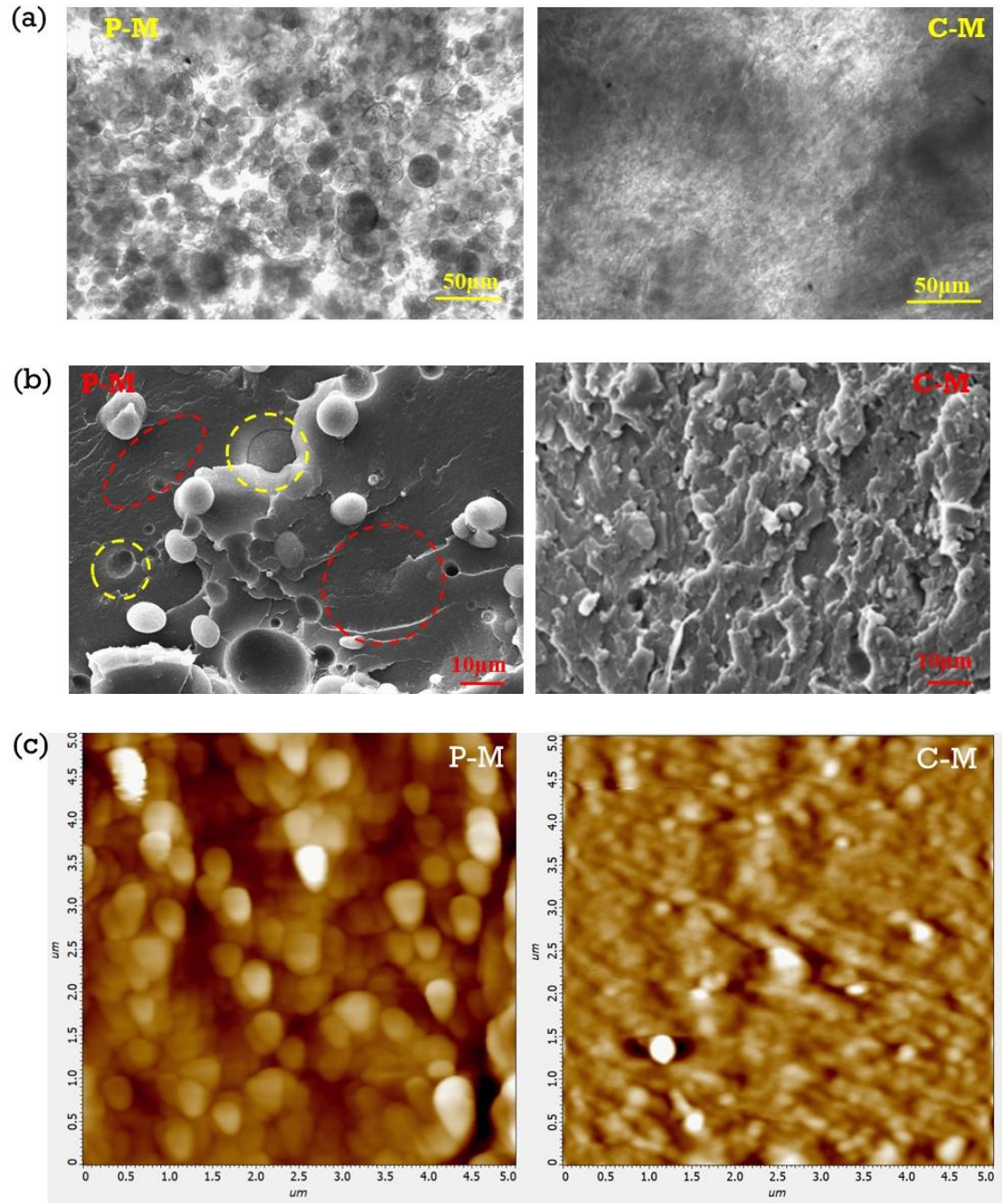

Figure 6.4: (a) *POM images of physical mixture (P–M) and chemical mixture (C–M) of ABS and PE;* ***(b)*** *SEM images of P-M and C-M, yellow dotted circles in the SEM image of P-M shows the embedded ABS particle in the PE matrix and the indentation left by ABS particle, red dotted circles represent the plain fractured surface of PE having no or fewer cracks*

present; and ***(c)*** *AFM images of P-M and C-M showing relative roughness of surfaces of blends.*

It is clearly seen from the SEM images that the P-M has a distinct two-phase morphology where the ABS particles are dispersed homogeneously in polyethylene matrix. The two phases are debonded, as shown in figure through circles. This debonding occurs due to low interfacial interaction between the two immiscible polymers. The poor miscibility arises due to different polarity of the two polymers. However, the two polymers are highly immiscible causing the separation of ABS particles in the form of spherical blobs in polyethylene matrix. On contrary, the chemical mixture (C-M) exhibits clear single-phase morphology. There is co-continuous type morphology present in C-M. The presence of MA creates crosslinking through reactive extrusion which convert it in a single-phase morphology.

The smooth surface with fewer cracks represents the effortless debonding in the P-M while rough fracture surface in C-M indicates better adhesion between the two components. Therefore, the developed C-M system has better morphological properties as compared to physical mixture due to chemical crosslinking [6, 8]. AFM is a tool to understand the roughness of the samples along with morphology. It is useful in determining the topographic or morphological changes as it can examine the morphology at very high spatial resolutions and area of micrometers to sub-nanometers can be scanned to examine the topography. The AFM images of 5 × 5 μm2 area of P-M and C-M have been shown in ***Figure 6.4c***. P-M shows globular morphology with the surface having distinct particle like impressions distributed all over the surface, further demonstrate the immiscible ABS particles in PE matrix in the blend. On the other hand, the chemical mixture shows the smoother surface comparatively. The morphology does not show the distinct particulate patterns in the C-M

as evident from the surface roughness of 16.5 nm as opposed to overall surface roughness of 24.7 nm in P-M. The smoother surface results from the chemical bonding caused by the crosslinking between ABS and PE through reactive extrusion in presence of maleic anhydride. Hence, the crosslinking structure during reactive extrusion diminished the immiscibility or in other words enhanced the miscibility of two incompatible polymers like ABS and PE [5].

6.3.2 Gel content through solvent extraction (indicative crosslinking density, CD*i*)

The solvent extraction has been performed to determine the gel content which gives the extent of crosslinking in the samples. ***Figure 6.5a*** shows the photographic images of P-M and C-M specimens before and after the solvent extraction (in chloroform, solvent for ABS) and xylene (solvent for PE)) with remaining weight percentage after each step. The samples of physical mixture are put in chloroform for 24 h. After 24 h, the samples are taken out from the chloroform and dried thoroughly. The weight difference before and after dipping in chloroform results in 14% weight reduction. After drying, the samples are put in xylene at a temperature of 140 °C under stirring condition. All the samples get dissolved in the solvent within 5 min. This signifies that there is no crosslinking in the prepared physical mixture. The chloroform dipping results in only 14 wt% of the ABS removal from P-M present on the surface. Remaining ABS is surrounded mostly by PE which chloroform could not dissolve. When the samples are put in xylene, they get dissolved in xylene despite having the tiny ABS particle in it. On the other hand, the chemical mixture which contains 5 wt% MA are also put in the respective solvents of both the polymers for 24 h each. After chloroform dipping for 24 h, the weight difference is ~9%. After that the samples are dipped in xylene. The samples do not dissolve completely, rather 45% of the initial weight remains.

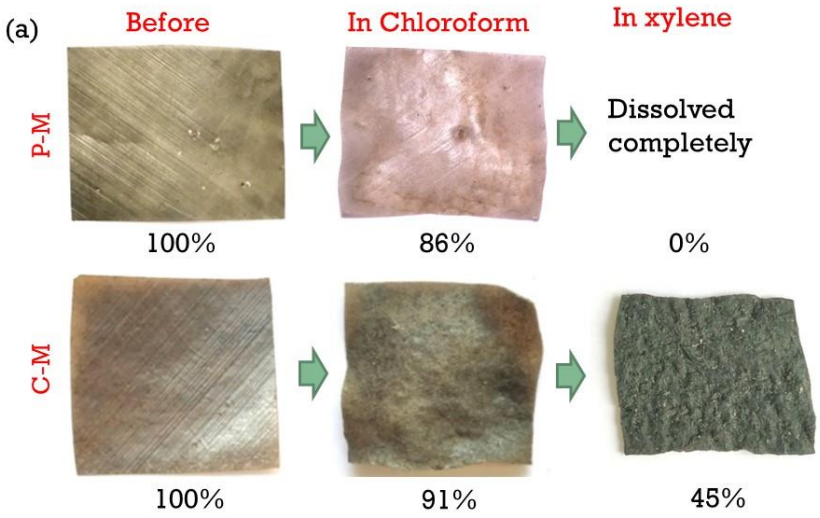
(a)
Before
In Chloroform
In xylene
P-M
Dissolved completely
100%
86%
0%
C-M
100%
91%
45%

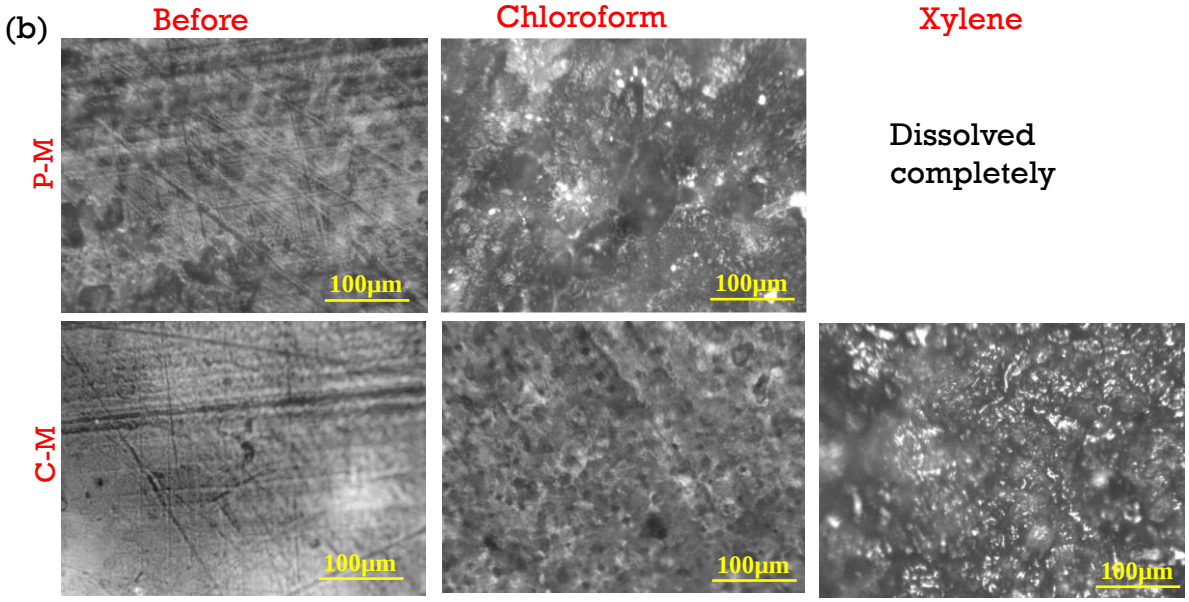
(b)
Before
Chloroform
Xylene
P-M
Dissolved completely
100µm
100µm
C-M
100µm
100µm
100µm

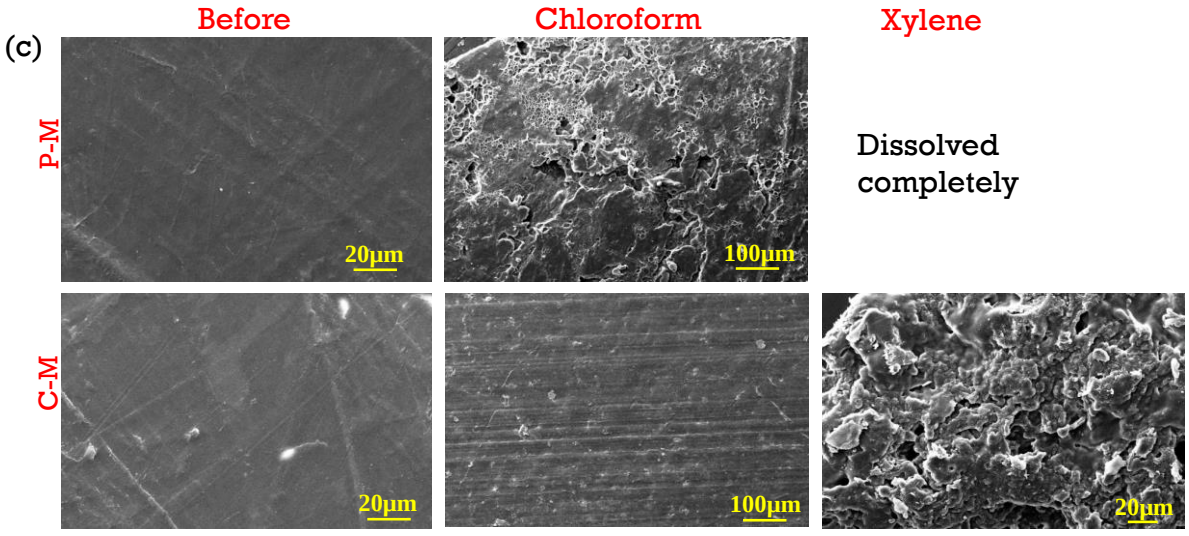
(c)
Before
Chloroform
Xylene
P-M
Dissolved completely
20µm
100µm
C-M
20µm
100µm
20µm

Figure 6.5: (a) *Photographic images of samples before and after the indicated solvent extraction, below each image, the percentage weight remained after each solvent extraction is mentioned;* ***(b)*** *Optical microscopic images in reflectance mode of the samples before and after solvent extraction; and* ***(c)*** *SEM images of samples before and after solvent extraction.*

This signifies that there is chemical bonding (crosslinking) between the two polymers due to which the resulting blend does not dissolve completely and the remaining undissolved 45% is considered as the extent of crosslinking in C-M blend. The images of samples before and after each solvent extraction have been shown in ***Figure 6.5b*** and ***6.5c*** through optical images and SEM, respectively. Polarized optical microscopic images have shown the visible pitting in P-M sample after solvent extraction using chloroform and the sample gets dissolved completely after putting in xylene. The C-M blend, however, shows less surface pitting as compared to P-M sample. The C-M specimen does not dissolve completely rather show considerable erosion of the surface due to solvent extraction using chloroform and xylene. SEM images in ***Figure 6.5c*** also show the similar surface morphologies of samples of P-M and C-M before and after solvent extraction. The surface of samples before solvent dipping is quite uniform. After putting the P-M blend in chloroform, it shows rough and uneven surface because of the erosion of ABS from the surface while it gets dissolved completely in xylene.

The sample of C-M also has an even surface before any solvent extraction while fewer pittings are observed after dipping in chloroform. It is clear that the surface erosion in C-M specimen is distinctly lesser than the P-M sample. The surface of C-M becomes more rough and uneven after dipping the sample in xylene because of 55% extraction of the polymers.

However, solvent extraction studies confirm the crosslinking in C-M in presence of maleic anhydride as opposed to the complete dissolution of physical mixture.

6.3.3 Proof of crosslinking and determination of its site

Morphology and solvent extraction studies indicate the possible crosslinking between the components (PE and ABS) and spectroscopic techniques are employed to visualize the chemical bonding. ***Figure 6.6a*** shows the FTIR spectroscopic patterns of pure polymers and their physical and chemical blends. Polyethylene shows the characteristic peaks at 2914 and 1462 cm^{-1} corresponding to the C–H stretching and bending of normal alkene, respectively. The peak at 718 cm^{-1} signifies CH_2 rocking [7]. The FTIR spectra of ABS show a stretching band of C≡N group at 2236 cm^{-1}. The ring modes of styrene show peaks at 1600 cm^{-1} and 1492 cm^{-1}. The peak at 1451 cm^{-1} is due to the scissoring mode of CH_2 groups. Peaks at 965 $cm^{-1}$and 909 cm^{-1} arise due to the C–H deformation of the hydrogen attached with the alkene carbons. These distinct peaks are taken as the representatives of butadiene component. The peaks appear at 758 and 698 cm^{-1} signify the intense ring bending [241] and no change of peak positions is observed in physical mixture confirm insignificant interactions between the components, which led the system to immiscible one. On contrary, a new FTIR peak at 1768 cm^{-1}appears in chemical blend (C-M), corresponds to the carbonyl group due to the presence of maleic anhydride, indicating possible linking of PE and ABS through MA. There is another new peak in C-M at 1015 cm^{-1} which corresponds to the C–O–C linkage [242]. These two new peaks indicate that the maleic anhydride form the crosslinking with the base polymers. Further, there are considerable shift of peak positions in C-M as compared to their respective pure polymers and P-M such as the peaks at 965 cm^{-1} shifts to 967 cm^{-1}, the intense ring bending peaks at 758 and 697 cm^{-1} shift to 759 and 699 cm^{-1}. All these shifts

signify the enhanced interactions between the two polymers in the chemical blend and turn into a single phase in maleic anhydride induced crosslinked blend.

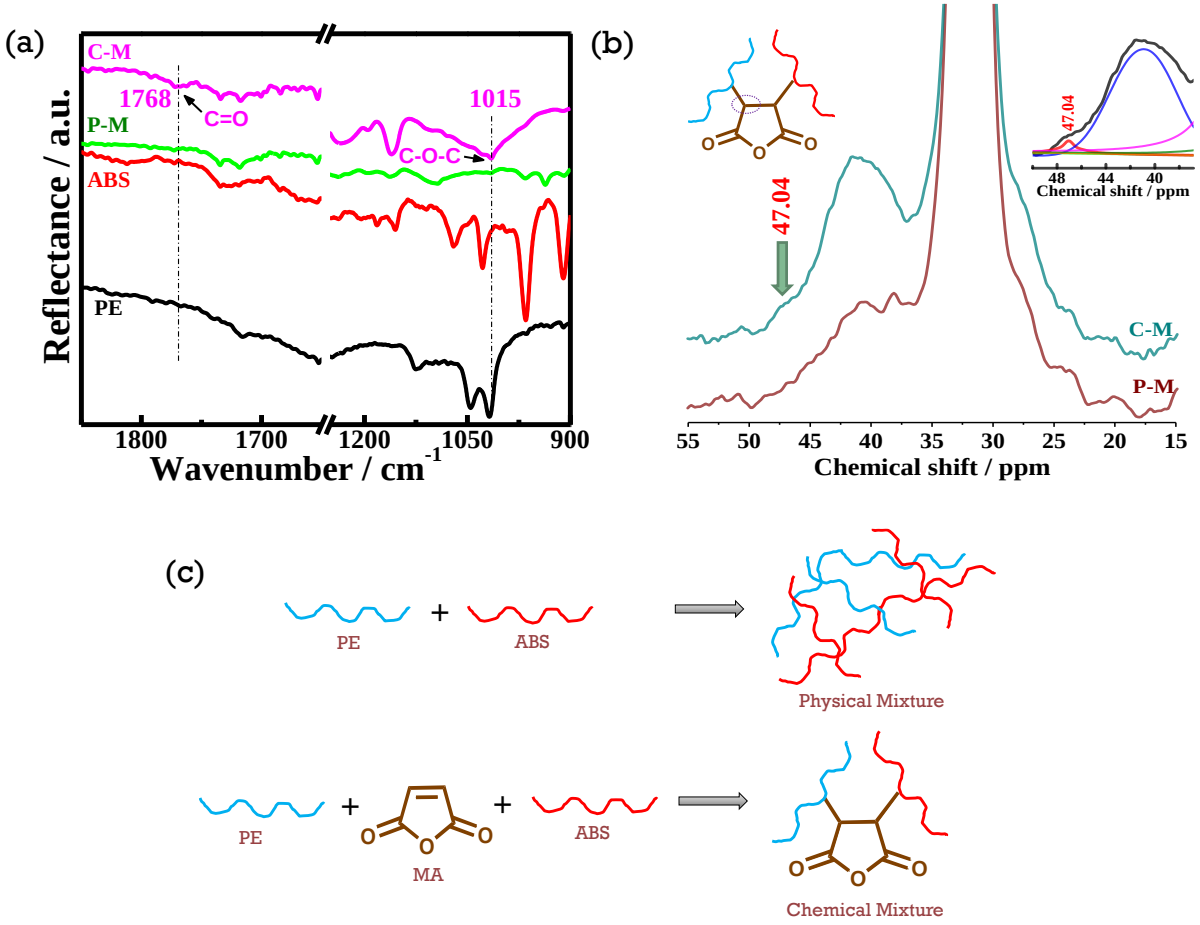

Figure 6.6: *Chemical bond formation due to reactive extrusion as determined through spectroscopic techniques,* ***(a)*** *FTIR spectra of indicated samples, vertical lines show the bands corresponding to chemical crosslinks;* ***(b)*** *solid state 13C NMR; downward vertical line indicate the position of new peak and corresponding carbon site of crosslinking is presented on top left, inset figure on right shows the deconvolution of the peak showing prominent peak at 47.04 ppm, (for FTIR and NMR of C-M, solvent extracted parts of C-M were used); and* ***(c)*** *reaction scheme showing overlapping molecules in P-M while MA induced crosslinking is shown in C-M.*

Figure 6.6b shows the solid state ^{13}C NMR spectra of physical and chemical mixture. A new signal at 47.04 ppm appears in C-M which is not present in physical mixture. This peak is deconvoluted to get the exact peak position as shown in the inset of ***Figure 6.6b***. This signal has emerged due to the attachment of MA with the main chains in the form of succinic anhydride as shown in inset of ***Figure 6.6b*** (the carbon atom to which the peak at 47.04 is assigned has been marked by the dotted circle) [243]. However, the chemical crosslinking in presence of maleic anhydride is confirmed through spectroscopic techniques indicating the position of carbon site of crosslinking between PE and ABS through MA. The reaction mechanism of physical and chemical blends have been shown in ***Figure 6.6c***, where only physical intermixing of molecules occur in P-M while crosslinking between PE and ABS ensue through maleic anhydride in the phases and thereby enhance the interfacial interaction through reactive extrusion [244, 245].

6.3.4 Thermal properties

To remove the thermal history, the samples are first heated from room temperature to 200 °C at a heating rate of 10°/min followed by quenching at a cooling rate of 40°/min. The second heating was then performed at a heating rate of 10°/min. ***Figure 6.7a*** shows the DSC thermograms and the values obtained from DSC studies are presented in ***Table 6.1***.

PE sample shows a melting peak at 108.5 °C while the physical mixture indicates a melting point at 107 °C, and the decreases of melting temperature is due to dilution effect. The solvent extracted crosslinked portion was used for the DSC measurement of C-M. The melting of C-M occurs at 105.5 °C. E-waste ABS shows a glass transition temperature (T_g) at 106 °C and its presence is unnoticeable as it merges with the melting temperature of blends. Melting

point of CM is lower than the P-M due to the rigid structure in crosslinked state. The formation of three dimensional structures may hinder the crystallization [8].

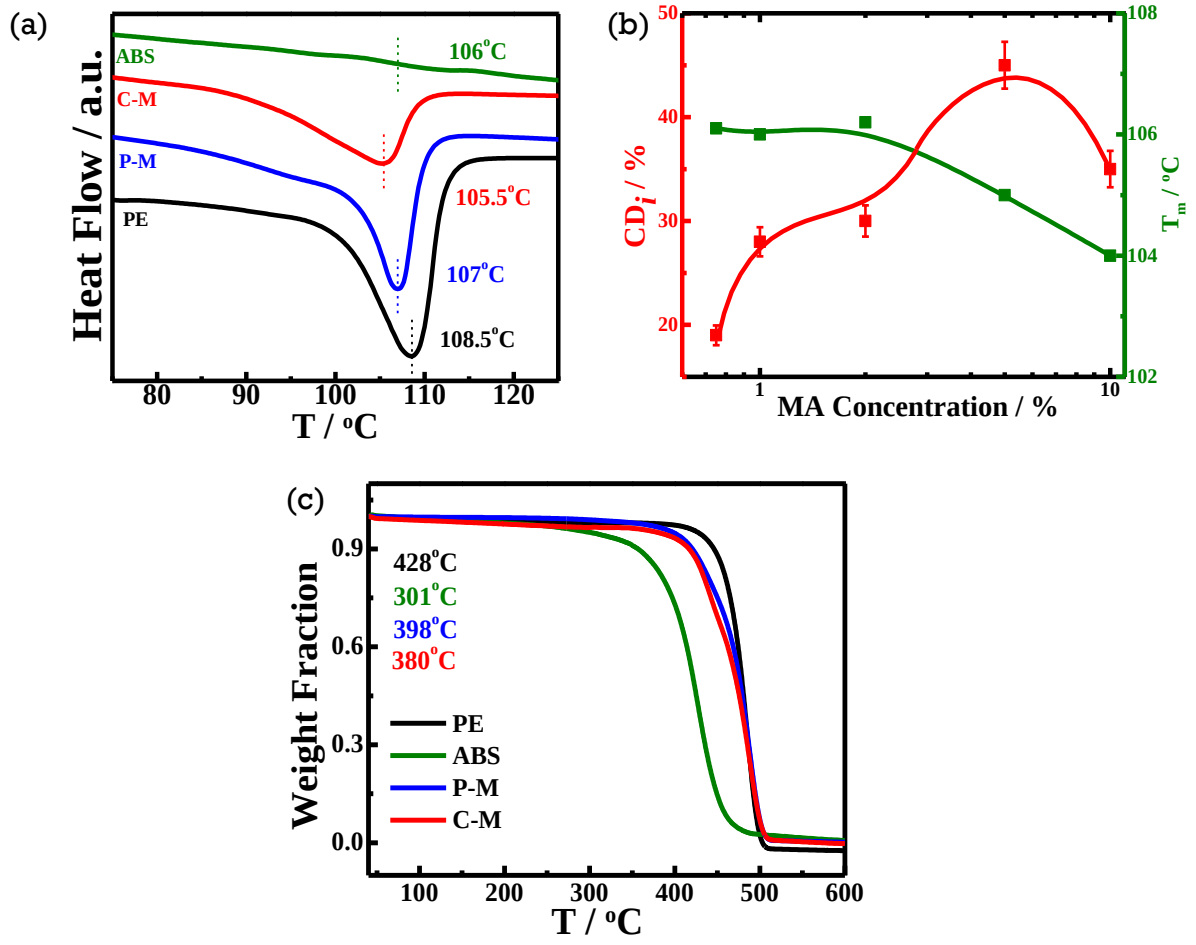

Figure 6.7: (a) *DSC thermograms of pure polymers and their indicated blends showing melting temperature;* ***(b)*** *indicative crosslink density (CD_i) and melting temperature of chemical mixture/ blends as a function of MA content; and* ***(c)*** *TGA thermograms of pure polymers and their indicated blends, degradation temperatures (T_d) correspond to 5% weight loss of samples.*

The crosslinked structure may restrain the growth of spherulites for the uniform arrangement of the crystalline content. Imperfect crystal formation could also contribute in the slight decrement of the melt temperature [246-249]. ***Figure 6.7b*** shows the effect of MA

concentration on the extent of crosslinking and melting temperature. The crosslink density, as measured from dissolution studies, increases with the concentration of MA in the blends and the maximum crosslinking is achieved 45% using 5 wt% of MA whereas the melting behavior follow a decreasing trend.

Table 6.1: *Melting temperature (T_m) and degradation temperature (T_d) obtained through DSC and TGA studies.*

Sample	**T_m (ºC)**	**T_d (ºC) (at 5% weight loss)**	**T_d (ºC) (at 50% weight loss)**
PE	108.5	428	478
ABS	-	301	422
P-M	107.0	398	476
C-M	105.5	380	473

The TGA thermograms of samples are shown in ***Figure 6.7c***. The degradation temperature (T_d) is taken as the temperature at which 5% weight loss occurs. Pure PE shows the T_d at 428 °C and ABS degrades at 301 °C. The degradation temperature of P-M and C-M are found to be 398 °C and 380 °C, respectively, considerably higher than pure ABS. The P-M has 25 wt% ABS contributing in the decrement of the thermal property of the physical mixture. The chemical mixture shows further decrement in degradation temperature. This degradation is unlikely and may have resulted from the chain scission reactions and degradation of unreacted MAH in the C-M. At 50% weight loss, pure PE shows T_d at 478 °C whereas the P-M and C-M has T_d at 476 °C and 473 °C, respectively. The T_d of P-M and C-M is comparable to the pure PE, denoting that thermal stabilities of P-M and C-M are comparable

with that of the PE. Presence of ABS in blends causes this slight compromise in the T_d as the ABS has T_d as low as 422 °C at 50% weight loss. The chain scission reactions taking place in C-M cause 3 °C drop in comparison to the P-M. ***Table 6.1*** shows the quantitative values of melting and degradation temperature.

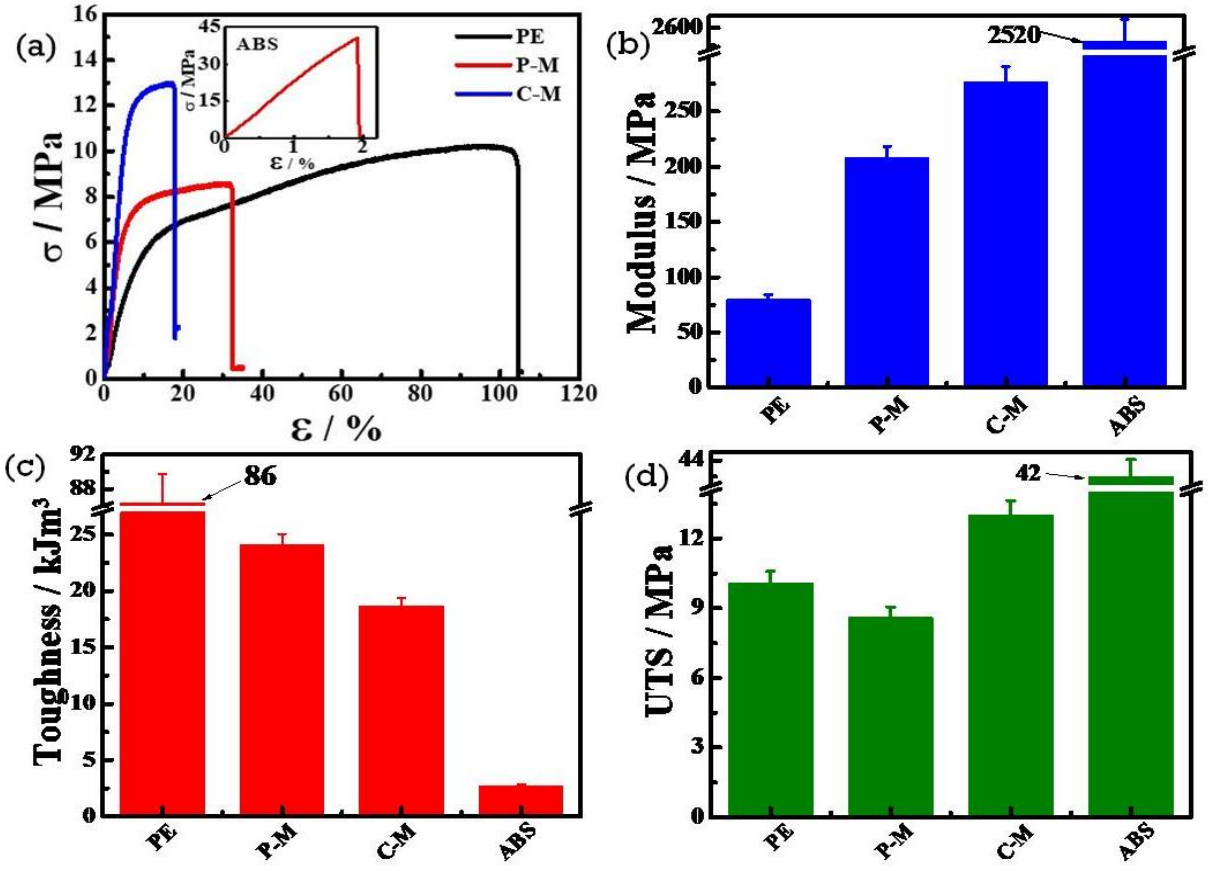

Figure 6.8: *Mechanical properties of pure polymers and their blends,* ***(a)*** *stress strain curves of PE, P-M and C-M, inset figure shows the stress strain curve of E-waste ABS;* ***(b)*** *modulus;* ***(c)*** *toughness; and* ***(d)*** *ultimate tensile strength (UTS) of indicated specimens.*

6.3.5 Mechanical properties

For the usage of blends in various applications, their mechanical performance was needed to be investigated. ***Figure 6.8a*** shows the stress-strain curve of PE and its indicated blends.

Young's modulus, toughness and ultimate tensile strength have been shown in ***Figure 6.8b, c*** and ***d***, respectively. The quantitative values of mechanical properties have been shown in ***Table 6.2***. The physical mixture shows an increment in the modulus value and considerable decrement of toughness and ultimate tensile strength.

Table 6.2: *Mechanical properties of pure polymers and their blends.*

Sample	**Young's Modulus (MPa)**	**Ultimate Tensile Strength (MPa)**	**Toughness (kJm^{-3})**	**Elongation at break (%)**
PE	80.1 ± 4.0	10.1 ± 0.5	86.3 ± 4.3	104.5 ± 5.2
ABS	2.50×10^3 ± 126.1	42.4 ± 2.1	2.7 ± 0.1	2.1 ± 0.1
P-M	208.1 ± 9.8	8.6 ± 0.4	24.1 ± 1.2	32.6 ± 1.6
C-M	276.8 ± 10.4	13.0 ± 0.6	18.6 ± 0.9	17.7 ± 0.8

On the other hand, the chemical mixture shows enhanced mechanical properties in terms of modulus and tensile strength. Toughness of C-M shows comparatively lower values as compared to PE and P-M, presumably due to lower elongation at break in crosslinked system as usual. It is noticed that modulus of P-M shows increased value of Young's modulus as compared to PE which is attributed to the inclusion of the ABS in the PE. ABS has high modulus and low toughness. The elongation at break of ABS used is as low as ~2%. The ABS particles are dispersed in PE matrix which influence the modulus of the physical mixture as the modulus of ABS is comparatively higher than PE. The embedded ABS

particles strengthen the P-M until the debonding between the two phases takes place. Although, the elongation at break of P-M decreases from 104.5% to 32.6% and toughness decreases to 18.6 kJm^{-3} from 86.3 kJm^{-3} of PE. The reason for the decrement of the elongation at break of P-M is the non-uniform distribution of ABS particles in the PE matrix. Uniform dispersion and size of the dispersed phase are critical criterion for the plastic deformation in the rubber toughened polymer blends [250]. The inclusion of non-homogeneous and critically large particles results in brittle failure at the interface of the two polymers in the polymer blend. The size of the particles of the dispersed phase should not be more than a critical limit. In SEM images of fractured surface of P-M (***Figure 6.4b***), it can be seen that the ABS phase was non-homogeneously dispersed in the PE matrix. The size distribution of ABS particles was very uneven. These two factors contributed in the low values of strain at fracture. Gupta et al. [163] also related the critical domain size of the dispersed phase to the toughening of the polymer blend and reported the decrease in the elongation at break of blend at the increasing content of ABS in PP/ABS blend. Bonda et al. [152] also observed the decrease in elongation at break due to the critical parameters of the dispersed phase. The morphology of fractured surface also revealed that the ABS particles were pulled out from the PE matrix at the interface. This debonding occurred as a result of the poor interfacial adhesion. The ABS particles were pulled out from the PE matrix mostly without being broken or fractured. They left the PE polymer interface leaving a clear indent, indicating the smooth debonding. It suggests that as the P-M started to stretch, both PE and dispersed ABS. But ABS has much less toughness as compared to PE. This difference results in the uneven stretching which created void between the two phases. The void formation led to the debonding of PE from the ABS particles' surfaces. As voids grew in size with increasing strain, the cracks developed and travelled through the blend. These cracks

culminated the ultimate failure of the physical mixture. The earlier crack generation compromised the tensile strength of the physical mixture which dropped to 8.6 MPa as compared to 10.1 MPa in PE. The chemical mixture shows the further increment in the modulus which is 246% higher than PE and 33% higher than P-M. The ultimate tensile strength of the C-M also increases to 13 MPa from 10.1 MPa of PE. The higher modulus attributes to the improved and homogeneous morphology of the C-M due to reactive blending. The ABS phase does not have the separate particles like morphology in C-M as it has in P-M. The SEM micrographs of C-M (***Figure 6.4b***) showed a uniform miscible structure which did not have two separate phase morphology. The interaction and miscibility between two phases increase significantly in the presence of MA. The reactive extrusion of C-M cause partial crosslinking in the blend which results in the stiffened network structure in a portion of C-M. This network structure contributes in the higher modulus values in C-M. The tensile strength also increases slightly in C-M unlike physical mixture where early debonding of ABS particle and PE causes decrement in tensile strength. The elongation at break, however, decreases more than the physical mixture which is primarily due to crosslinking [6, 152, 251]. The reason behind this behavior may also lie on the chain scission reactions taken place in the crosslinked blend [252]. Due to the chain scission and stiffened structure because of crosslinking, the network structure shows decreased strain at fracture and toughness. ***Figure 6.9*** depicts the three point bending test results of PE and its blends. The flexural stress strain curve, flexural stress and flexural modulus values have been presented in ***Figure 6.9a, b*** and ***c*** respectively. The bending properties of the blends are found to be improved significantly. The flexural stress increases slightly in P-M while significant improvement is noticed in P-M. The quantitative value of flexural stress of pure

PE is 7.0 MPa which has increased to 8.5 MPa (21%) in P-M. On the other hand, C-M shows an increment of 83% of flexural stress value (12.9 MPa).

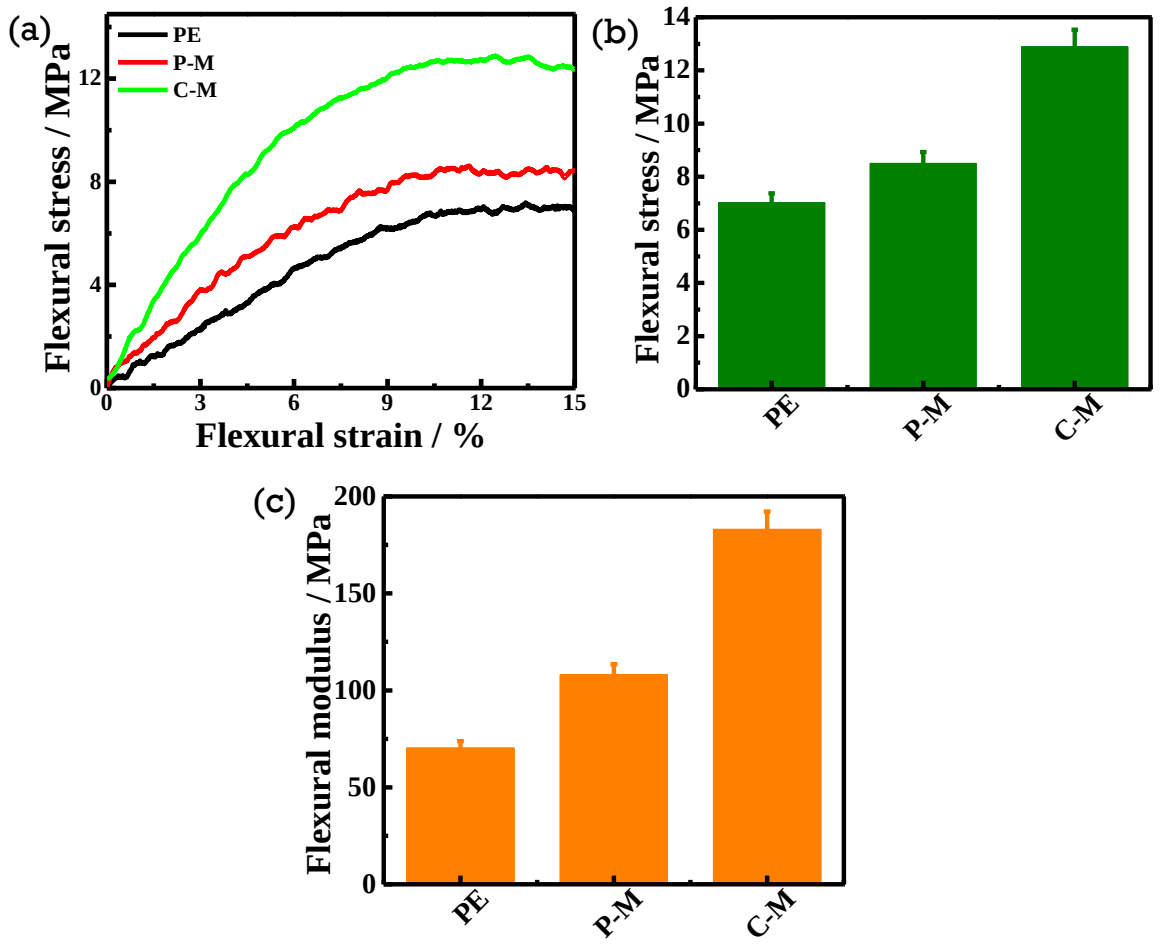

Figure 6.9: *Three point bending test results of PE, P-M and C-M* ***(a)*** *flexural stress-strain curves;* ***(b)*** *comparative flexural stress; and* ***(c)*** *flexural modulus showing relative increment in physical and chemical blending.*

The flexural modulus also shows the similar behavior. The P-M exhibits an increment of 53% in the flexural modulus whereas addition of MA results in 160% improvement of flexural modulus in C-M. The developed chemical blend shows superior bending properties upon the addition of MA in minute quantity. The enhancement in bending properties is attributed to the crosslinking achieved through reactive extrusion in presence of MA. The

crosslinked structure provides stiffness in C-M which results in the excellent flexural properties. P-M shows very little increment because of the poor interfacial properties between PE and ABS phase as observed in morphological studies. Therefore, it is corroborated that C-M has excellent mechanical performance to be used for various practical applications.

6.3.6 Dynamic Mechanical Analysis (DMA)

The Mechanical properties under dynamic condition as measured through DMA provide storage modulus, loss modulus and loss tangent as a function of temperature (***Figure 6.10 a, b*** and ***c***). The storage modulus is indicative of the elastic modulus whereas the loss modulus illustrates the energy lost. The damping factor (tanδ) is calculated through the ratio of loss modulus to the storage modulus. The storage modulus variation with temperature has been shown in ***Figure 6.10a***. The G /of C-M shows increased values as compared to PE and P-M. The P-M shows decrement in storage modulus at low temperatures presumably due to immiscible interphase structure while miscible structure in C-M helps improving the stress transfer to occur smoothly. The curve of ABS shows that the storage modulus of ABS is the highest because of its high stiffness. The storage modulus results are in support of the elastic modulus data. The loss modulus variation with temperature has been presented in ***Figure 6.10b***. The two peaks represent α and β phases of LDPE. The peak at higher temperature (55 °C) represents the α phase which is indicative of motion of chains in the crystalline region. The peak at lower temperature (−27 °C) represents the β phase, which is associated with the molecular motion of chains in amorphous region [253]. The temperature of peak of β phase is considered as glass transition temperature [254]. Pure ABS, however, does not have these transitions with temperature variation and has a constant value curve of loss modulus till 70

°C. Due to presence of ABS phase in both the blends, amorphous part increases because of which the peak of β phase persist in P-M as well as in C-M.

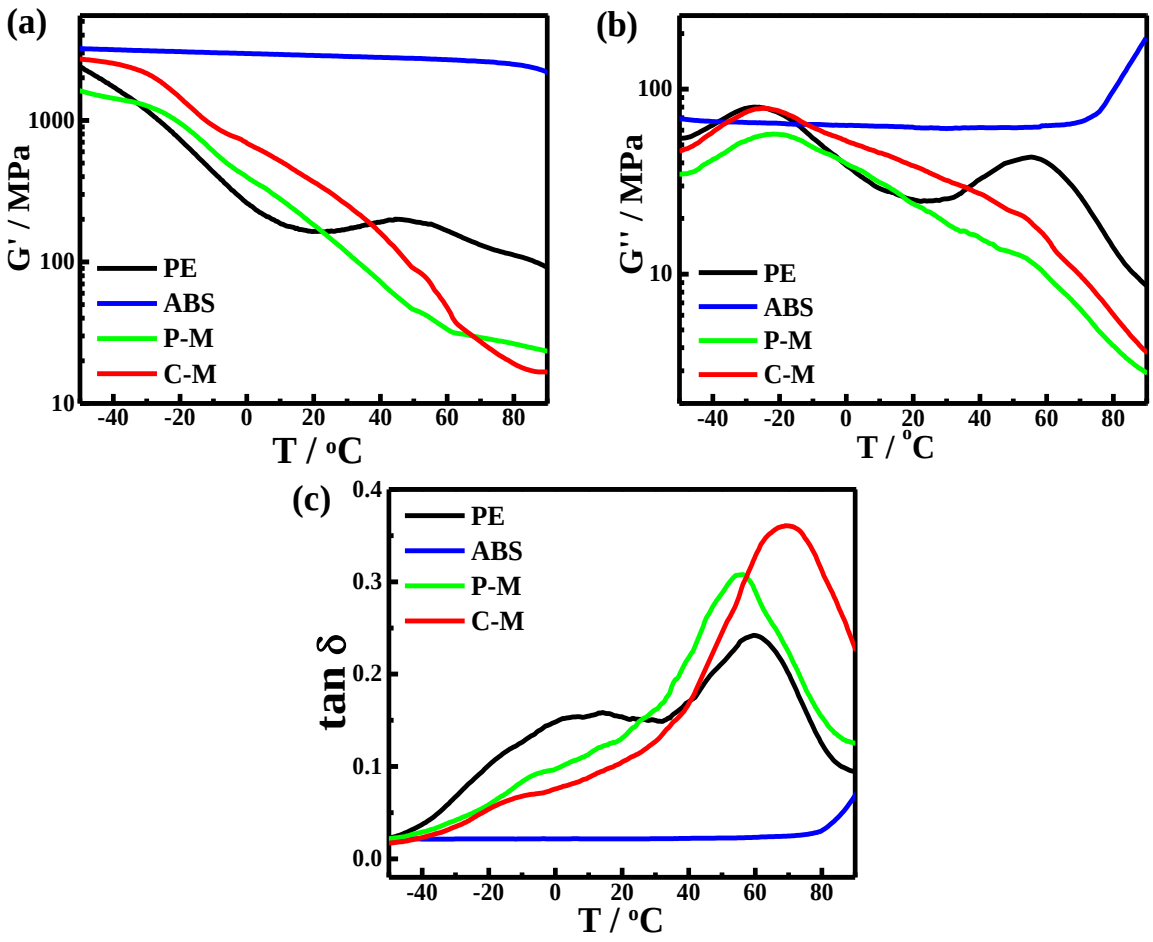

Figure 6.10: *Dynamic mechanical analysis of PE, its indicated blends and ABS; variation of* ***(a)*** *storage modulus;* ***(b)*** *loss modulus; and* ***(c)*** *tanδ of indicated specimens as function of temperature.*

The crystalline content decreases considerably, hence, the peak of α phase gets suppressed in P-M and C-M. The tan δ (loss tangent) being the ratio of loss and storage modulus, represents the contribution of both viscous and elastic parts of the material. The α peak appears in PE at 60 °C which shifts to higher temperatures in C-M. In P-M the peak temperature decreases to 55 °C but the intensity of peak increases. In C-M the peak

temperature increases to 70 °C and the intensity of peak also increases. The intensity increment results due to the restriction in the movement of the polymer chains. In P-M, this restriction is posed by the embedded ABS particles. The peak intensity increases further in C-M due to the enhanced rigidity caused by greater restrictions in the polymer chains due to crosslink network present in the chemical blend which hinders the free movement considerably [253-255].

6.3.7 Heat distortion temperature (HDT)

The HDT is the ability to resist the significant physical deformation against temperature under load. It is a crucial parameter for the product designing as dimensional stability during the practical applications and can be affected by the thermal conditions. Hence, the polymer blends are tested at elevated temperature to determine the maximum temperature at which the blends are dimensionally stable.

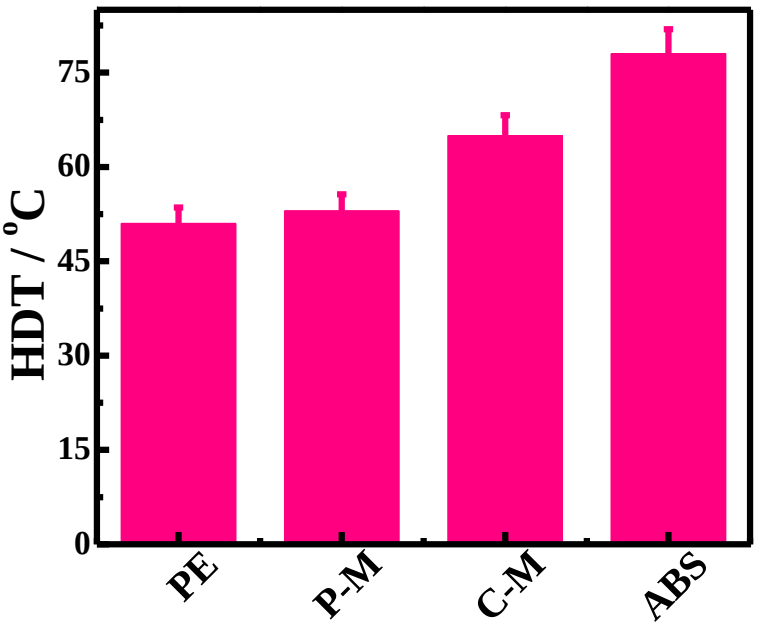

Figure 6.11: *Heat distortion temperature of PE, its indicated blends and ABS.*

Figure 6.11 shows the results of the heat distortion temperature. Pure PE shows a HDT of 51 °C and ABS polymer showed HDT of 78 °C. The P-M is almost as stable as PE having HDT at 53 °C. However, the HDT of C-M is found to be well above PE and P-M at 65 °C. Therefore, it is deduced that under thermal effect, the C-M shows better dimensional stability and is the most suitable for practical applications. Chemical blend in presence of maleic anhydride (C-M) exhibits significant mechanical properties as compared to physical mixture primarily due to the crosslinking of the constituent polymer molecules and thereby forming a homogeneous structure.

6.4 Conclusion:

The chemical mixture of LDPE and ABS have been prepared via one step reactive extrusion in a twin screw extruder in presence of 5 wt% maleic anhydride. C-M has shown enhanced properties due to the formation of crosslinked structure. SEM, POM have been used to examine the phase structural changes in crosslinked C-M. A single-phase morphology has been observed in chemical blend as comparison to two phase morphology in physical mixture prepared in absence of MA. AFM has also confirmed the change from two phase morphological structure to single phase morphology in chemical mixture. The surface roughness has been found to be decreased, indicating formation of smoother surface. Gel content has been determined via solvent extraction to observe the indicative crosslinking density. Inclusion of 5% MA found to impart the maximum crosslinking in the C-M. The structure of C-M has been examined using FTIR and solid state NMR. There are changes and shifting in the peaks of FTIR and NMR spectra which corroborates the strong chemical interactions in the chemical mixture. The chemical mixture has been found to be thermally stable although it has showed a lower degradation temperature. The Young's modulus

increases up to 246% in C-M as comparison to pure PE and 33% in physical mixture. Tensile strength shows an increment of 29% in P-M as compared to pure PE. Flexural properties have also been improved and an increment of 160% has been found in flexural modulus and 83% in flexural stress. The C-M has showed 27% increment in heat distortion temperature which can be a crucial parameter in practical application where exposure of heat is prerequisite. This work has demonstrated a one-step reactive extrusion process to enhance the properties of widely used e-waste (ABS) and LDPE. Therefore, the prepared C-M has shown a way to utilize the discarded plastic by circulating it again in a useful and superior manner.